Project No: 603502

DACCIWA

"Dynamics-aerosol-chemistry-cloud interactions in West Africa"

Deliverable

D1.5 Combined data analysis, conceptual model development and model evaluation

Due date of deliverable:	30/11/2018
Completion date of deliverable:	30/11/2018
Start date of DACCIWA project:	1st December 2013 **Project duration:** 60 months
Version:	[V1.0]
File name:	[D1.5_Model_evaluation_DACCIWA_v1.0.pdf]
Work Package Number:	**1**
Task Number:	**3**
Responsible partner for deliverable:	**KIT**
Contributing partners:	**UPS, UNIVLEEDS, KNUST, OAU**
Project coordinator name:	Prof. Dr. Peter Knippertz
Project coordinator organisation name:	Karlsruher Institut für Technologie

The DACCIWA Project is funded by the European Union's Seventh Framework Programme for research, technological development and demonstration under grant agreement no 603502.

Dissemination level		
PU	Public	**x**
PP	Restricted to other programme participants (including the Commission Services)	
RE	Restricted to a group specified by the consortium (including the Commission Services)	
CO	Confidential, only for members of the consortium (including the Commission Services)	

Nature of Deliverable		
R	Report	**x**
P	Prototype	
D	Demonstrator	
O	Other	

DOCUMENT INFO

Authors

Author	Beneficiary Short Name	E-Mail
Fabienne Lohou	UPS	Fabienne.lohou@aero.obs-mip.fr
Norbert Kalthoff	KIT	norbert.kalthoff@kit.edu
Bianca Adler	KIT	Bianca.adler@kit.edu
Karmen Babic	KIT	karmen.babic@kit.edu
Cheikh Dione	UPS	Cheikh.dione@aero.obs-mip.fr
Marie Lothon	UPS	Marie.lothon@aero.obs-mip.fr
Maurin Zouzoua	UPS	Maurin.zouzoua@aero.obs-mip.fr
Xabier Pedruzo Bagazgoitia	UPS	Xabier.pedruzobagazgoitia@wur.nl

Changes with respect to the DoW

Issue	Comments

Dissemination and uptake

Target group addressed	Project internal / external
Scientific	Internal and external

Document Control

Document version #	Date	Changes Made/Comments
V0.1	24.10.2018	Template with basic structure
V0.2	13.11.2018	First complete version for approval by the DACCIWA general assembly
V1.0	30.11.2018	Final version approved by the DACCIWA general assembly

Table of Contents

1 Introduction

This deliverable aims at presenting the conceptual model for the low level cloud (LLC) diurnal cycle in southern West Africa and the relevant processes involved, built from the analysis of the DACCIWA dataset. More precisely, the conceptual model has been established based on the results from Adler et al. (2018), Babic et al. (2018) and Dione et al. (2018) who analysed the Savè super site (Benin) data set. It was verified that the main results obtained at the Savè site were also valid at the two other super sites of the DACCIWA campaign (Kumasi/ Ghana and Ile-Ife/Nigeria).

2 Sites and Data

The low level cloud formation during the night is a very common phenomenon in southern West Africa as can be seen in Figure 1. During the DACCIWA field campaign (June-July 2016), cloud observations at the 55-synoptic stations network pointed out an occurrence ranging between 40 and 100% and cloud coverage above 5 octas.

15 Intensive Observation Periods (IOPs) were operated during the DACCIWA field campaign at the three super sites. During these IOPs, in addition to the continuous measurements, some frequent radio-soundings were launched every 1 to 3 hours (depending on the super site) between 1800 UTC to 1200 UTC the day after, covering a large part of the low level cloud diurnal cycle. The results presented hereafter are largely based on the analyses of the IOP days.

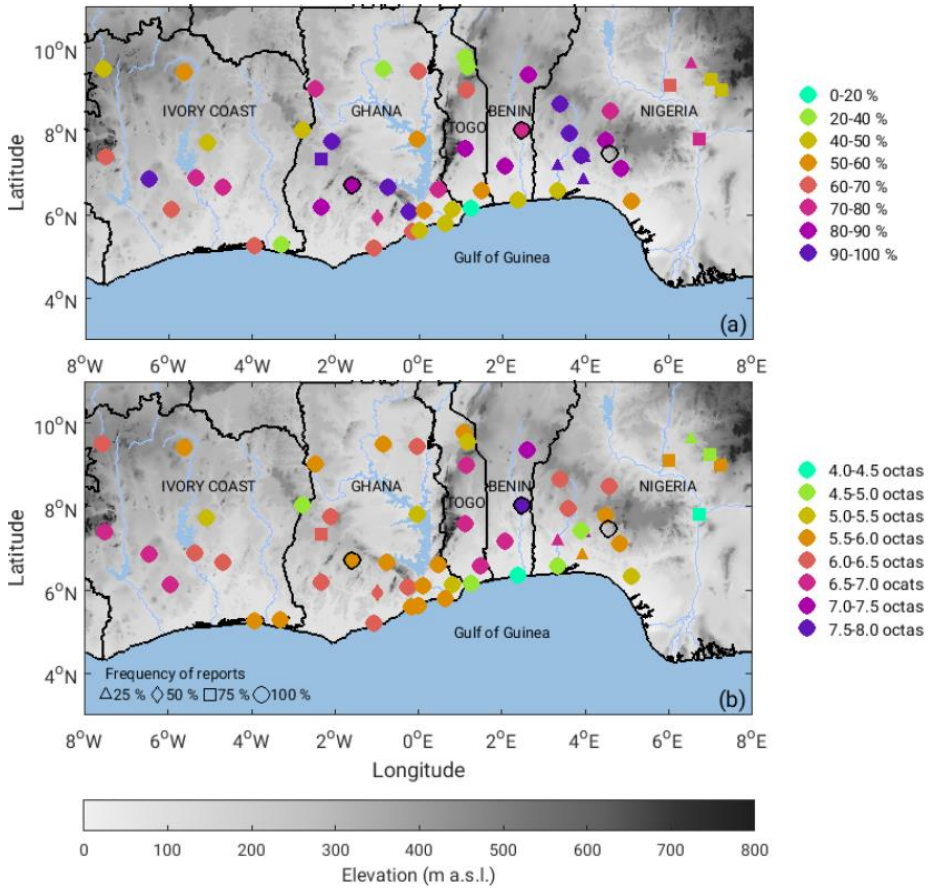

Figure 1: Topography (grey shading) of southern West Africa with superimposed (color scale) (a) occurrence and (b) cloud fraction of stratiform clouds reported at the synoptic 55-station network at 0600 UTC during the DACCIWA field campaign (14 June-31 July 2016). Only stratiform clouds with more than 4 octas coverage are considered in the statistic. Frequency of reports (shape of the markers) indicates the percentage of days with available data during the whole period. The three super sites, Kumasi in Ghana, Savè in Benin and Ile-Ife in Niger, are indicated with black circles.

3 Conceptual Model

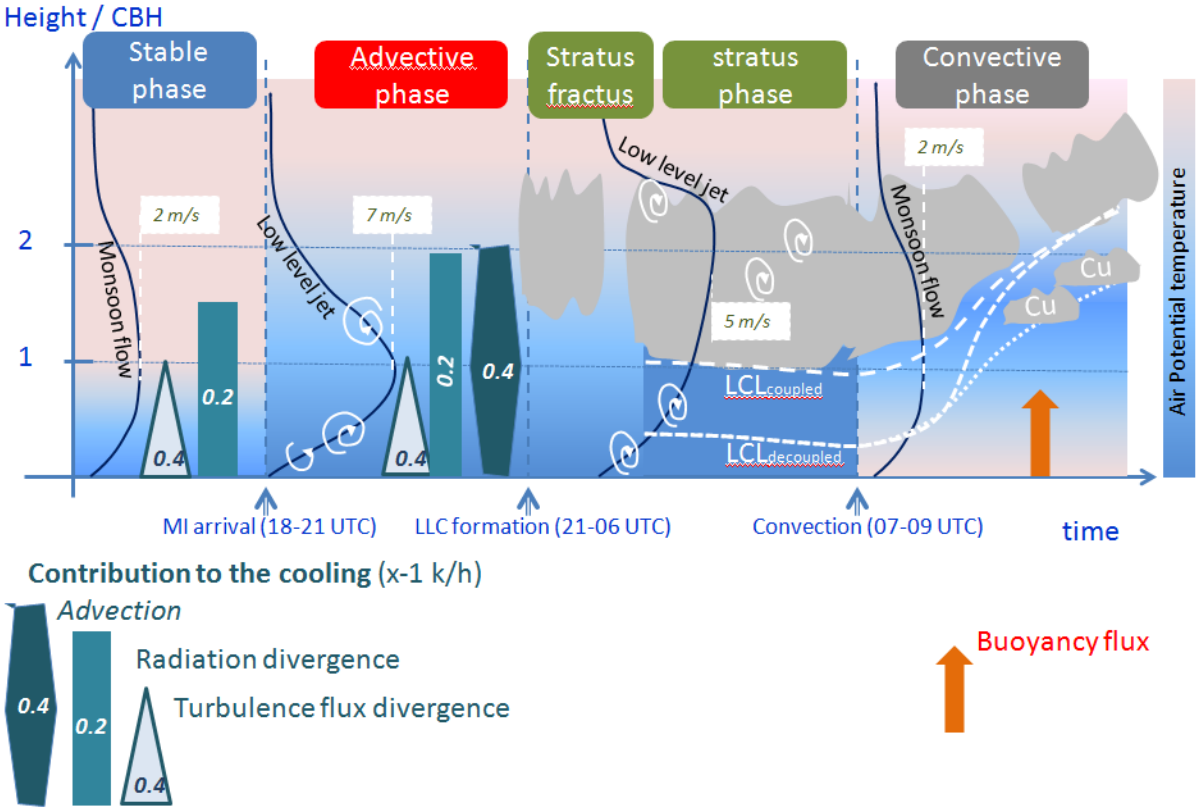

Figure 2: Conceptual model for the LLC diurnal cycle in southern West Africa. The height is normalized by the LLC base height (CBH) when the cloud forms. The grey shades represent the LLC or cumulus cloud (when indicated). The white dashed curves indicate the lifting condensation level. The blue line stands for the vertical profile of the wind with indication of its maximum value. The blue-filled rectangles and triangles schematize the processes involved in the potential temperature equation.

The diurnal cycle of the low level cloud is divided in five phases. A short presentation of the different phases is given in this paragraph (Figure 2). The first phase, named stable phase, starts in the end of the afternoon. During that phase, the monsoon flow is weak and the thermal convection vanishes. A stable layer forms close to the surface. The second phase is named the advective phase. It starts with the Maritime Inflow[1] arrival at the site and is characterized by the nocturnal low level jet settlement. Stable and advective phases are key phases since the processes which take place during that period lead to an increase of the relative humidity up to saturation. We will present in the following sections the processes responsible for this relative humidity increase. The third phase starts when the low level cloud forms. In some cases, a stratus fractus deck (stratus fractus phase) forms before the appearance of a more homogeneous deck (stratus phase). During these cloudy phases, strong interactions exist between the cloudy layer and the sheared wind of the low level jet. At last, the fifth phase corresponds to the start of the thermal convection and the vertical development of the boundary layer. The different scenarios for the LLC breakup will be presented in the following sections.

[1] Because of the close location of the DACCIWA super sites (~180 km) from the Guinean coast, the sites are affected by coastal phenomena. During the day, an advection of oceanic air mass over the continent (sea-breeze) is superimposed onto the monsoon flow. The propagation of this air mass is slowed by the turbulence in the continental boundary layer during the day. At the end of the afternoon, the convection vanishes and this air mass can propagate farther inland, advecting cooler air. This late afternoon phenomenon is called the Maritime Inflow.

4 The five phases of the LLC diurnal cycle

A detailed description of each of the phases and a presentation of the main physical processes occurring during each phase are given in this section.

The five phase's characteristics are presented in Figure 3, which is composed of 15 height-time sections of wind speed, potential temperature, specific humidity, relative humidity and bulk Richardson number. Theses 15 panels are built by hourly averaging the frequent radio soundings launched at Savè supersite and by normalizing the height by the cloud base height (CBH) when the stratus forms. On the first column, the origin of time is set to the Maritime Inflow arrival time (Dione et al., 2018): the negative and positive times stand for stable and advective phases, respectively. On the second column, the origin of time is set to the stratus formation time: the negative and positive times stand for stratus fractus and stratus phases, respectively. On the right column, the origin of time is set to the start of convective phase: the whole panel is then for the convective phase.

4.1 Before cloud formation

The phases under focus in this section are the ones before the cloud formation: stable and advective phases. During these phases the atmospheric conditions change to reach saturation.

4.1.1 Description of the stable and advective phases

The description of the stable and advective phases is based on the left column of Figure 3.

A weak monsoon flow persists during the end of the afternoon during the stable phase. The low layer stabilizes with an increase of the Richardson number because of the decrease of the temperature near the ground. But no clear change in relative humidity is observed during the stable phase.

The advective phase starts when the Maritime Inflow reaches the site. The low level jet usually sets in shortly after. These two combined advections imply a progressive increase of the wind up to 10 m s^{-1} at the end of the advective phase, right before the cloud formation. The jet core height is located at Z/CBH = 1. At the same time a cooling occurs in the layer between Z/CBH = 0 and Z/CBH = 2, whereas no clear change in specific humidity is observed. These figures show that the observed increase in relative humidity is due to a cooling rather than a moistening of the atmosphere. An additional impact of the wind increase during the advective phase is the decrease of the Richardson number, particularly below Z/CBH = 1, due to the sheared layer below the jet core.

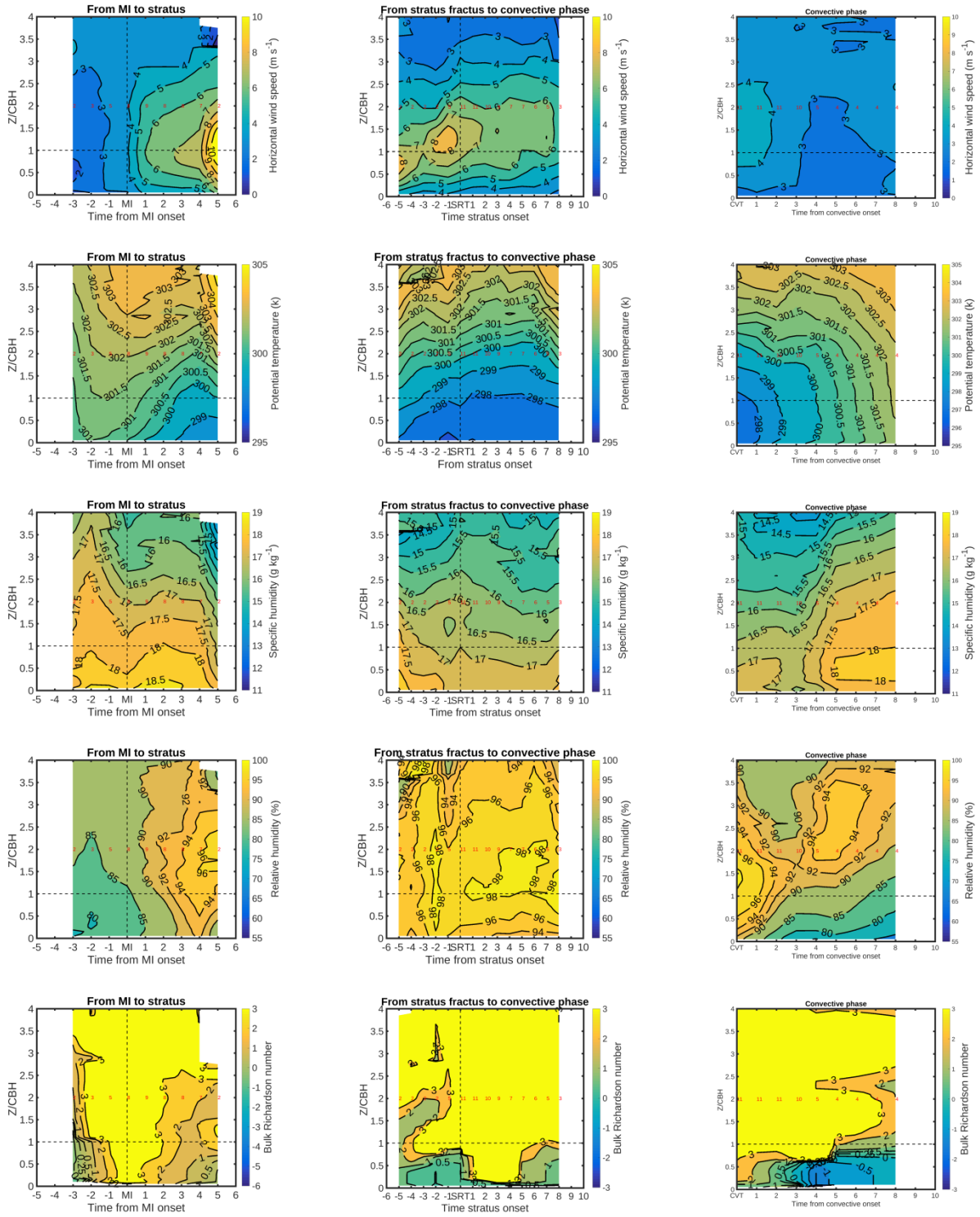

Figure 3: Mean height-time sections for, from top to bottom, wind speed, potential temperature, specific humidity, relative humidity and bulk Richardson number. These height-time sections are built by hourly averaging the frequent radio soundings launched at Savè supersite, and by normalizing the height by the cloud base height when stratus forms. Red numbers indicate the number of radio soundings available for the hourly-average. The origin of time is set to (left column) maritime inflow arrival time (negative and positive times standing for stable and advective phases, respectively), (middle column) stratus formation (negative and positive times standing for fractus stratus and stratus phases, respectively), and (right column) start of convective phase.

4.1.2 Relevant processes leading to saturation

The contributions of the cooling and the moistening to the relative humidity temporal change during the stable and the advective phases have been quantified (Adler et al, 2018, Babić et al., 2018). Figure 4 confirms that the cooling represents at least 80% of the change in relative humidity, with an even larger temperature contribution at Savè site. However, it is striking how the vertical profiles are similar at both sites, yet several 100 kilometres apart.

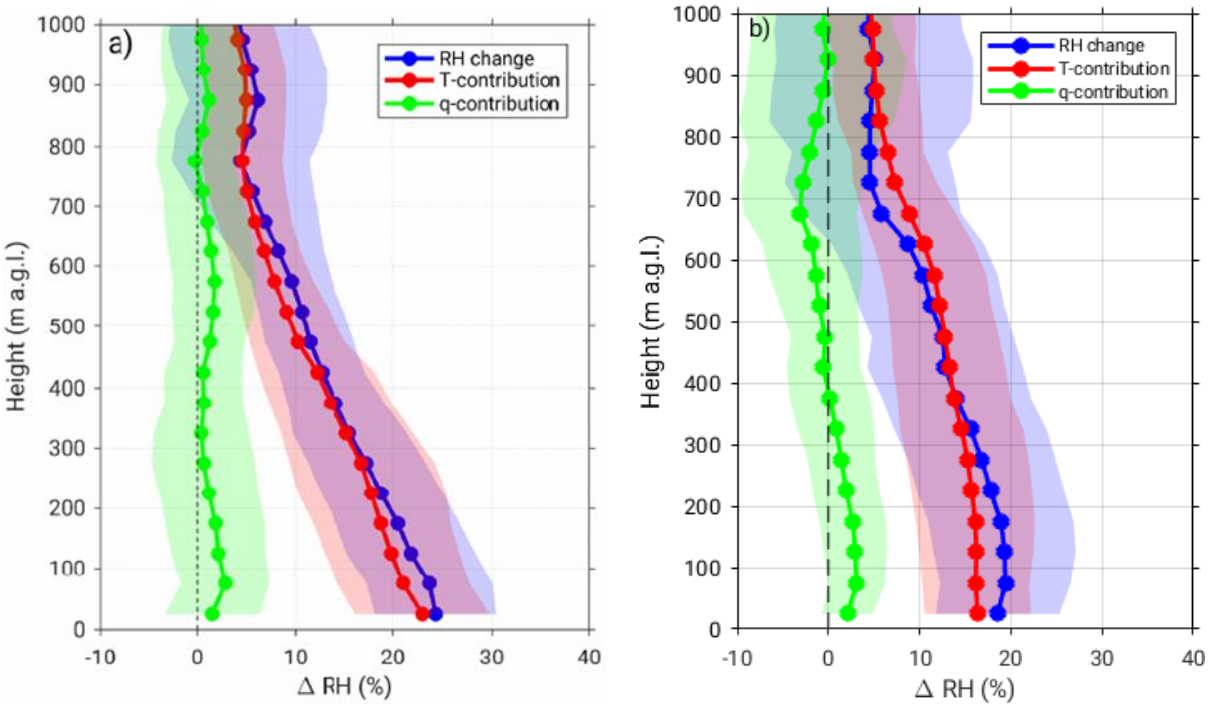

Figure 4: Specific humidity and temperature mean contributions to the mean total change in relative humidity at Savè (left panel) and Kumasi (right panel) averaged for all IOPs. The shading indicates the standard deviation.

The cooling being established as the main factor for the relative humidity increase, the processes responsible for the cooling are now investigated (Figure 5). The radiosondes launched at the super sites and those launched close to the Guinean coast allow us to estimate the total cooling rate during stable and advective phase and the contribution of the advective term in the potential temperature equation. The radiation divergence term is calculated with a radiative model (Adler, 2018, Babić et al., 2018). The residual term includes the vertical divergence of the sensible heat flux and the phases change terms. The latter being neglected before cloud formation, the residual term is mainly due to sensible heat flux divergence. Figure 5 (top panel) shows a total cooling that decreases with height from -0.8 K/h at surface to -0.2 K/h at 900m. The contribution of advection to the cooling is also height dependent with a vertical profile closely linked to the horizontal wind profile. The cooling by advection is then -0.2 K/h at surface and at 900 m height, with a maximum cooling of -0.4 K/h at the jet core height. The radiative divergence term contribution is found approximately constant with height and slightly below -0.2 K/h. This means that the flux divergence term is the main contribution to the cooling close to the ground, -0.4 K/h, with a decreasing effect with height, until it gets to zero at cloud base height. In conclusion, when integrating the vertical profiles with height, the advection is the main cooling process, responsible for 50% of the cooling of the atmosphere during the stable and advective phase. The two other terms (radiation and flux divergences) each contribute to 20% of the cooling. The bottom panel in Figure 5 presents the total cooling, the advection, radiation and residual contributions for each IOP.

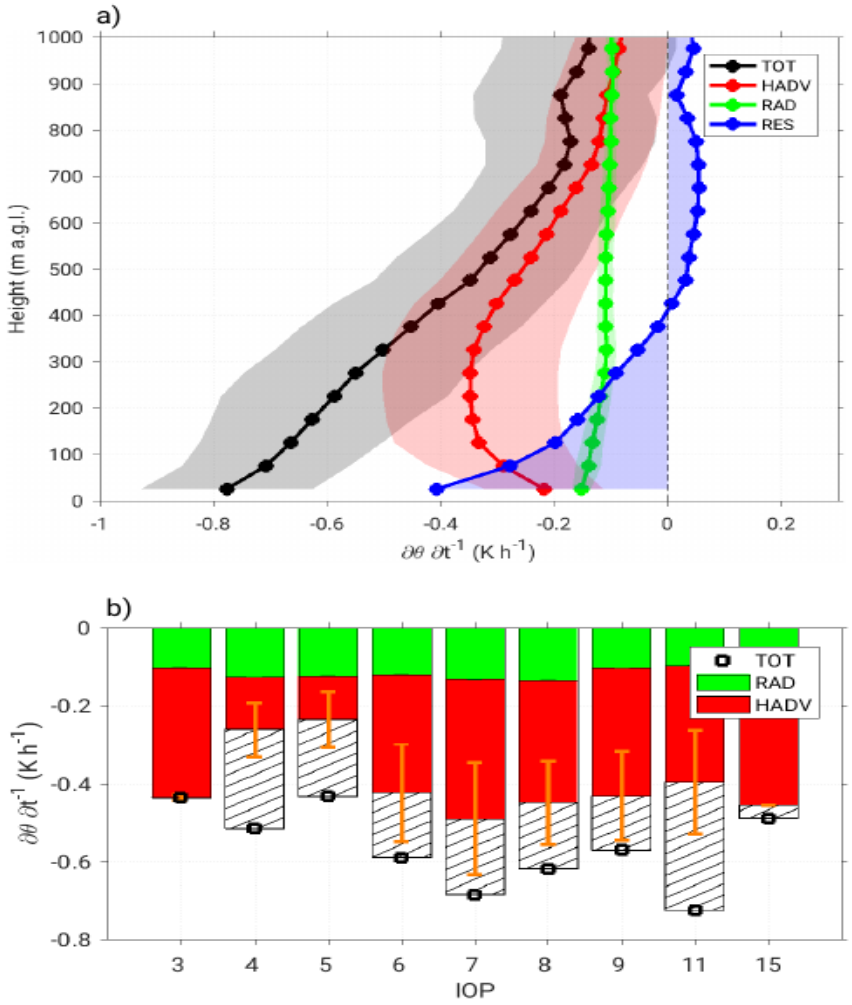

Figure 5: Vertical profiles of total cooling rate and contribution estimates of advection and radiative divergence terms for the Savè site. The residual term mainly represents the turbulent flux vertical divergence. The shading colored areas indicate the standard deviation. The bottom panel shows the vertically-averaged cooling rate and estimates of advection, radiative divergence and residual terms for each IOP

4.2 From cloud onset to cloud breakup

The three phases presented in this section are the two cloudy phases (stratus fractus and stratus) and the convective phase during which the LLC breakup occurs.

4.2.1 Description of the cloudy and convective phases

The middle column in Figure 3, presents the stratus fractus (negative times before the stratus deck formation) and the stratus (positive time) phases characteristics.

The highest values of the horizontal wind speed, defining the low level jet core, are observed around Z/CBH = 1 during the stratus fractus phase and until the beginning of the stratus phase. When the stratus deck forms, its base corresponds to the height of the low level jet core. This particular feature can be explained by the fact that the cooling by advection is the highest at this level. One hour after the stratus formation, the wind speed decreases and gets more constant with height between Z/CBH = 0.5 and Z/CBH = 2. The change in the wind vertical profile is due to the turbulent mixing in the cloudy layer. Although reduced, the maximum values of the wind are found within the cloudy layer during the stratus phase (Adler et al., 2018, Dione et al. 2018). The potential temperature in the subcloud layer is also homogenised by the shear-driven turbulence below the LLJ core.

The right column in Figure 3 presents the convective phase characteristics. This phase starts when the surface sensible heat flux exceeds 10 Wm^{-2}. The wind speed is back to monsoon flow daytime condition that is with weak wind of about 3 ms^{-1}. The potential temperature increases with time, and shows a well mixed layer above the instable surface layer. The relative humidity maximum expectedly rises with time, but is sometimes reduced (for example 3 hours after the start of the convective phase). These results highlight a cloudy layer that rises as the convective boundary layer develops and as the stratus low level cloud breaks (even if an average height-time section can hardly show this).

4.2.2 Relevant processes linking the cloudy layer to the surface

The shear-driven turbulence below the jet core has a major impact on the cloud formation and dissolution. A turbulent subcloud layer will couple the cloud layer to the surface, inducing a cloud base close to the lifting condensation level. On the contrary, a subcloud layer with very low turbulence will be mixed less. The cloud can then be decoupled from the surface and its base be higher than the lifting condensation level. This is shown in Figure 6 where the difference between the cloud base height and the lifting condensation level is plotted against the Richardson number in the subcloud layer.

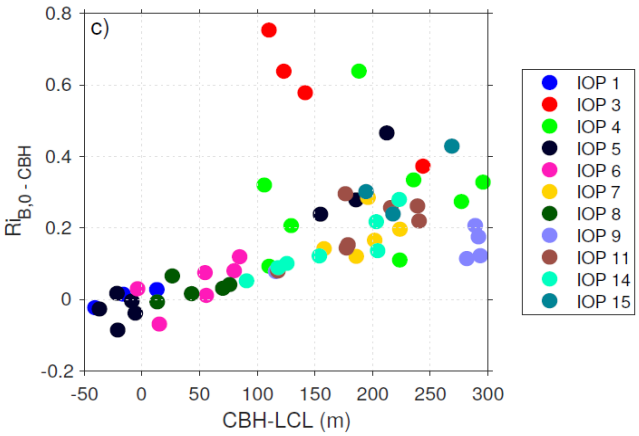

Figure 6: Richardson number in the subcloud layer according to height difference between cloud base height (CBH) and lifting condensation level (LCL). Colors stand for the difference IOPs.

The way the cloudy layer and the surface are coupled plays a determining role on the low level cloud breakup. Three scenarios have been observed at the Savè site, illustrated in Figure 7.

- The cloudy layer and the surface are coupled: the low level cloud base rises with the boundary layer vertical development (IOP 8, Fig. 7). The boundary layer height is estimated here using the lifting condensation level (LCL). This method is motivated by the very good accordance between the LCL and the cumulus cloud base which develop in the afternoon.
- The cloudy layer and the surface are decoupled:
    - the boundary layer height rises up to the cloud base (IOP 14, Fig. 7),
    - the boundary layer height rises but some cumulus clouds form at the top below the low level cloud (IOP 4, Fig. 7).

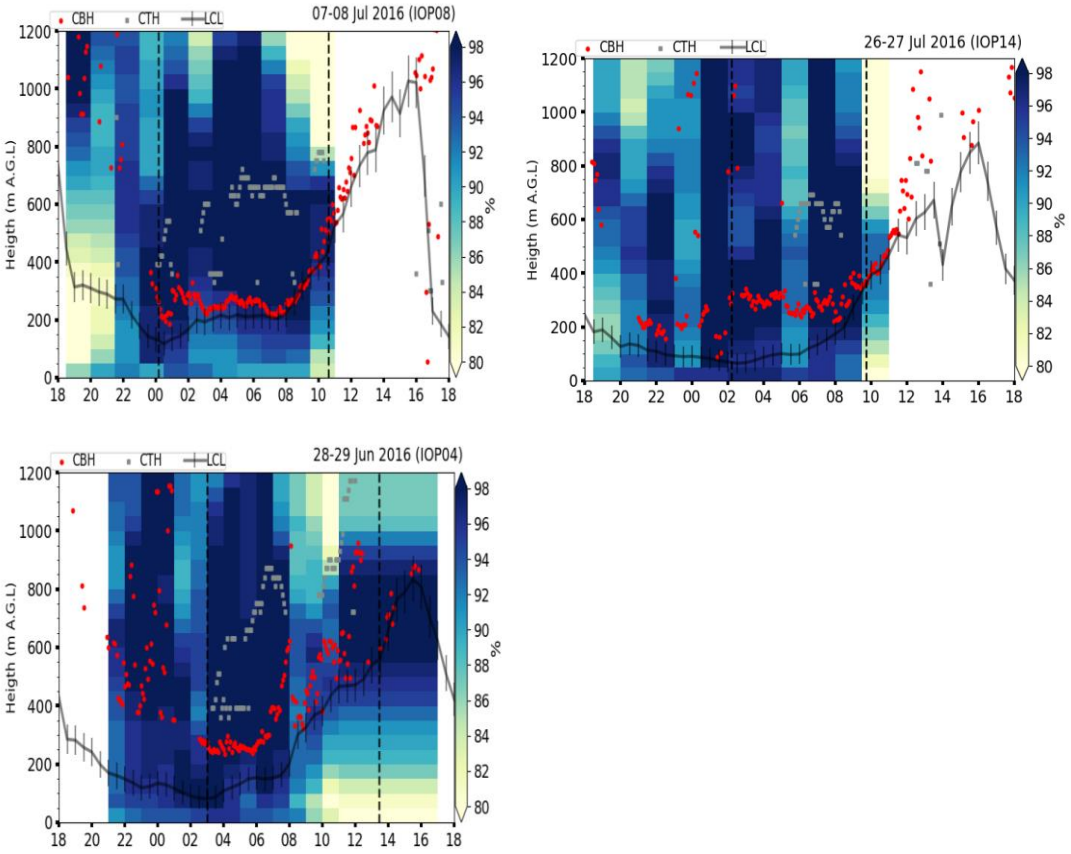

Figure 7: Temporal evolution of the LCL (dark line), LLC base (red dots) and LLC top (grey dots) for IOP 8 (top left), 14 (top right) and 4 (bottom). The color bar stands for relative humidity.

5 Impact of the low level cloud on the boundary layer development

The LLC breakup time (defined with the infrared camera) impacts the surface energy balance (SEB) during daytime conditions. Figure 8 presents the temporal evolution of the integrated terms of the SEB starting from sunrise (0530 UTC) until 1800 UTC, for the Savè and Kumasi sites. Some differences between the two sites can be noticed: 1) the Bowen ratio (that is the ratio of sensible heat over latent heat fluxes, H/Le) is around 1 in Kumasi and about 0.5 in Savè, 2) the net radiation is lower in Kumasi because the albedo is larger. A high variability of the integrated terms can be observed among the IOPs. Integrated net radiation varies from 5000 to 7500 Wm^{-2} at the end of the afternoon according to the IOP. The amount of energy either available at surface (Rn) or dissipated by the surface toward the atmosphere (H or Le) strongly depends on the LLC breakup time, as shown in Figure 8 (bottom left panel). The later the LLC breakup, the smaller the SEB integrated terms.

The decrease in buoyancy flux with subsequent LLC breakup has an effect on the convection in the boundary layer and the maximum height reached by the LCL (Figure 8).

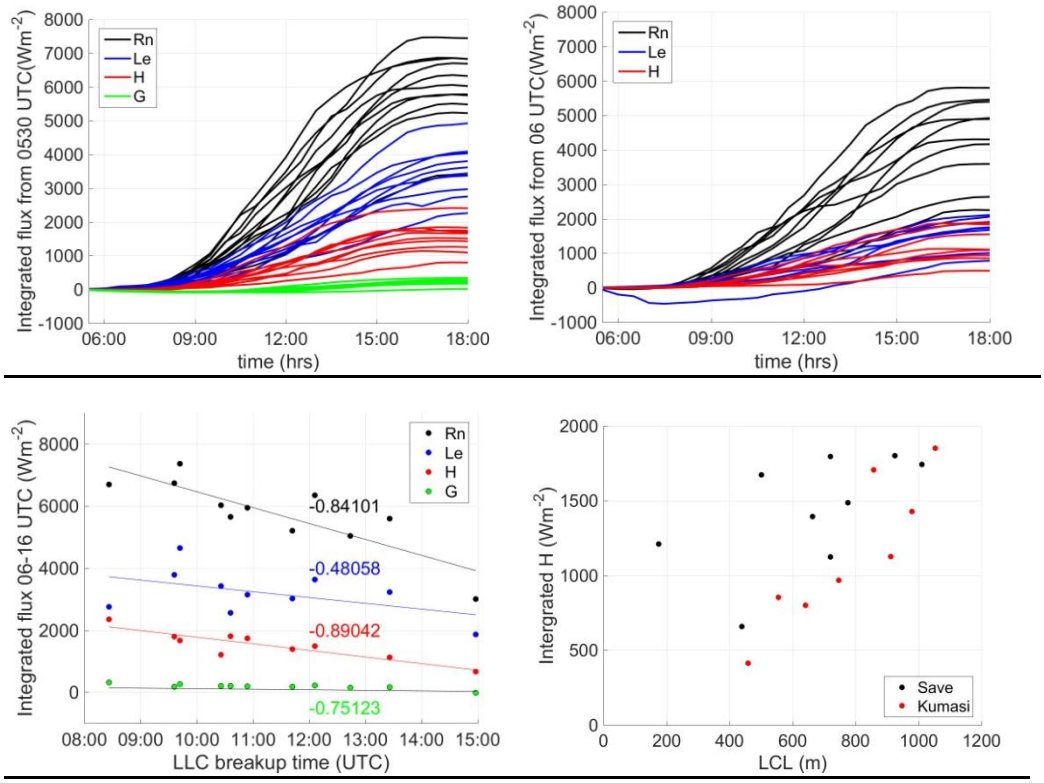

Figure 8: Integrated net radiation (Rn), latent (Le) and sensible (H) heat flux from 0530 UTC to 1800 UTC at (top-left panel) Savè and (top-right panel) Kumasi supersites. Each curve stands for one IOP. Integrated Rn, Le and H between 0530 and 1600 UTC against LLC breakup time at (bottom-left panel) Savè supersite. Integrated H between 0530 and 1600 UTC against LCL at 1600 UTC (bottom-right panel) at the Kumasi and Savè supersites.

6 Contribution of the Large Eddy Simulation to the conceptual model

A modelling study performed with Large Eddy Simulation (see Deliverable D01.4 by Xabier Pedruzo Bagazgoitia) aims at simulate the cloud thinning and break up transition during the day based on idealized conditions of the DACCIWA campaign. The simulated case is similar to the coupled cases we observed during the DACCIWA experiment (example of IOP8, Figure 7). The first results of the LES study shows the subtle equilibrium and the conditions needed to obtain a cloud layer and troposphere in equilibrium. This base simulation obtained, the on-going work consist in adding or changing processes shown to be relevant for the stratus cloud rising and breakup during the day. The processes (Figure 9) concern the solar radiation increase during the day, the surface fluxes, the wind shear at surface and at the entrainment zone. The quantification of the respective role of each process will help to better understand the differences between the three cloud-breakup scenarios observed during the DACCIWA experiment.

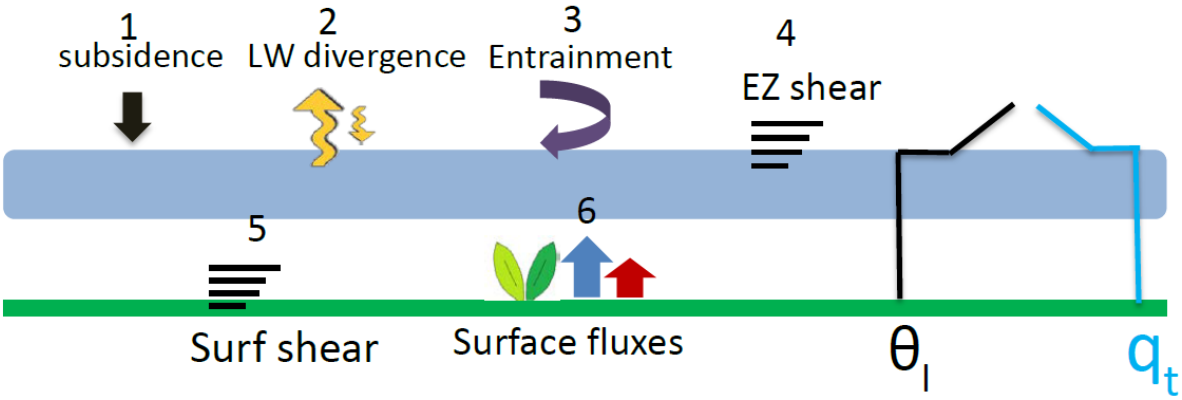

Figure 9: Schematic overview of local factors affecting the maintenance, evolution and dissipation of stratus/stratocumulus clouds. On the right, typical profiles for liquid water potential temperature and total water mixing ratios.

7 Conclusions

These results point out that the low level cloud formation and dissolution depend on the contribution and interaction of several processes, which makes the low level cloud simulation difficult. However, a central dynamical feature seems to be the Maritime Inflow combined to the nocturnal low level jet which partly drive the advection and the buoyancy flux divergence, both contributing to the cooling of the atmosphere before the cloud formation. The low level jet again plays an important role during the cloudy period of the night through the intensity of the shear-driven turbulence. The LLC has a strong impact on the SEB, reducing the buoyancy flux during daytime in case of late breakup. In that case the convection is reduced and the boundary layer height less vertically developed.

8 References

Adler, B., Babić, K., Kalthoff, N., Lohou, F., Lothon, M., Dione, C., Pedruzo-Bagazgoitia, X., and Andersen, H. (2018). Nocturnal low-level clouds in the atmospheric boundary layer over southern West Africa: an observation-based analysis of conditions and processes. *Atmospheric Chemistry and Physics. Discuss.* In review.

Babić, K., Adler, B., Kalthoff, N., Andersen, H., Dione, C., Lohou, F., Lothon, M., and Pedruzo-Bagazgoitia, X. (2018). The observed diurnal cycle of nocturnal low-level stratus clouds over southern West Africa: a case study. *Atmospheric Chemistry and Physics.* In Review.

Bessardon, G., Brooks, B., Abiye, O., Adler, B., Ajao, A., Ajileye, O., Altstädter, B., Amekudzi, L. K., Aryee, J. N. A., Atiah,W. A., Ayoola, M., Babi´c, K., Bärfuss, K., Bezombes, Y., Bret, G., Brilouet, P.-E., Cayle-Aethelhard, F., Danuor, S., Delon, C., Derrien, S., Dione, C., Durand, P., Fosu-Amankwah, K., Gabella, O., Groves, J., Handwerker, J., Kalthoff, N., Kohler, M., Kunka, N., Jambert, C., Jegede, G., Lampert, A., Leclercq, J., Lohou, F., Lothon, M., Medina, P., Pätzold, F., Pedruzo Bagazgoitia, X., Reinares, I., Sharpe, S., Smith, V., Sunmonu, L. A., Tan, N., and Wieser, A. (2018). A dataset of the 2016 monsoon season meteorology in southern West Africa - an overview from the DACCIWA campaign. *Scientific Data Paper.* In review.

Derrien, S., Bezombes, Y., Bret, G., Gabella, O., Jarnot, C., Medina, P., Piques, E., Delon, C., Dione, C., Campistron, B., Durand, P., Jambert, C., Lohou, F., Lothon, M., Pacifico, F., and Meyerfeld, Y. (2016). DACCIWA field campaign, Savè super-site, UPS instrumentation. *doi.org/10.6096/dacciwa.1618*.

Dione, C., Lohou, F., Lothon, M., Adler, B., Babić, K., Kalthoff, N., Pedruzo-Bagazgoitia, X., Bezombes, Y., and Gabella, O. (2018). Intra-seasonal evolution of the most important low-troposphere dynamical structures over Southern West Africa during DACCIWA field campaign. *Atmospheric Chemistry and Physics.* In Review.

Handwerker, J., Scheer, S., and Gamer, T. (2016). DACCIWA field campaign, Savè super-site, Cloud and precipitation. *doi.org/10.6096/dacciwa.1686*.

Kohler, M., Kalthoff, N., Seringer, J., and Kraut, S. (2016). DACCIWA field campaign, Savè super-site, Surface measurements. *doi.org/10.6096/dacciwa.1690*.

Kalthoff, N., Lohou, F., Brooks, B., Jegede, G., Adler, B., Babić, K., Dione, C., Ajao, A., Amekudzi, L. K., Aryee, J. N. A., Ayoola, M., Bessardon, G., Danuor, S. K., Handwerker, J., Kohler, M., Lothon, M., Pedruzo-Bagazgoitia, X., Smith, V., Sunmonu, L., Wieser, A., Fink, A. H., and Knippertz, P. (2018). An overview of the diurnal cycle of the atmospheric boundary layer during the West African monsoon season: results from the 2016 observational campaign. *Atmospheric Chemistry and Physics*, 18, 2913–2928.

Wieser, A., Adler, B., and Deny, B.: DACCIWA field campaign, Savè super-site, Thermodynamic data sets (2016). *doi.org/10.6096/dacciwa.1659*

9 Glossary

CBH: cloud base height

H: sensible heat flux

IOP: intensive observation period

Le: latent heat flux

LCL: lifting condensation level

LLC: low level cloud

MI: Maritime Inflow

NLLJ: nocturnal low level jet

Rn: net radiation